

The shape of the van der Waals loop and universal critical amplitude ratios

This article has been downloaded from IOPscience. Please scroll down to see the full text article.

1998 J. Phys. A: Math. Gen. 31 L629

(<http://iopscience.iop.org/0305-4470/31/37/002>)

View [the table of contents for this issue](#), or go to the [journal homepage](#) for more

Download details:

IP Address: 171.66.16.102

The article was downloaded on 02/06/2010 at 07:11

Please note that [terms and conditions apply](#).

LETTER TO THE EDITOR

The shape of the van der Waals loop and universal critical amplitude ratios

Michael E Fisher and Shun-yong Zinn†

Institute for Physical Science and Technology, University of Maryland, College Park, MD 20742, USA

Received 23 June 1998, in final form 10 July 1998

Abstract. Assuming that a van der Waals loop for a fluid, ferromagnet, etc, can be defined, its shape is analysed on the basis of universal critical amplitude ratios for three-dimensional Ising-type systems. Selected estimates for these ratios are tabulated. Near criticality, the loop attains a universal scaled form given, optimally, by a new parametric *extended sine model* for the bulk asymptotic equation of state; but a (particular) low-order interpolating Padé approximant provides a reasonable fit. Among other universal features, the reduced *spinodal* magnetization/density and conjugate field are found to be $(\bar{m}_s, \bar{h}_s) \simeq (0.697, -0.513)$ in contrast to the van der Waals values $(0.577 \dots, -0.384 \dots)$: thus the spinodal lies appreciably closer to the binodal (or coexistence curve) than predicted classically.

All classical, Landau, or mean-field equations of state for fluids, ferromagnets, etc, that predict a first-order transition exhibit also a characteristic van der Waals (vdW) loop which **(a)** extends through the full, equilibrium two-phase region, **(b)** represents an isothermal, real *analytic* continuation of the equation of state through the coexistence curve or phase boundary, and **(c)** approaches the simple cubic form $h \propto M[M^2 - M_0^2(T)]$ in the critical region, $t \equiv (T - T_c)/T_c \rightarrow 0^-$: here M denotes an appropriate order parameter, while $M_0(T) \approx B|t|^\beta$ is its spontaneous (or coexistence) value beneath T_c and h is the conjugate thermodynamic field. (For precise definitions here and below, see the appendix.) The vdW loop plays *no* role for thermodynamic states, even if spatially *nonuniform*, outside the coexistence curve, i.e. with, asymptotically, $M^2 \geq M_0^2(T)$. By contrast, in all classical theories of surface tension, interfaces, spinodal decomposition, etc (see, e.g. [1, 2]), the presence and properties of the loop are crucial. And this is true also of more general *local functional theories* [1, 3, 4] that allow for the observed *nonclassical* values of the critical exponents $\alpha, \beta, \gamma, \dots$. Accordingly, it is appropriate to consider the *shape* profile, $h(M)$, of a vdW loop more closely, especially, near criticality.

First, however, it must be stressed that the very *existence* of a full van der Waals loop is in doubt from the viewpoint of statistical mechanics. Thus, as regards point **(a)**, above, there exist exactly soluble microscopic models [5] in which, while an isotherm can be analytically continued into the two-phase region, the real continuation does *not* extend across to the other phase. More generally, for systems with normal interactions of finite

† Current address: Supercomputing Applications Laboratory, Samsung Advanced Institute of Technology, PO Box 111, Suwon 440-600, Republic of Korea.

range, the presence of *essential singularities* on the phase-boundary [5–8] precludes **(b)**, i.e. forbids *any* definition via analytic continuation.

While recognizing the power of these objections, we will adopt here the well sanctioned ‘traditional thermodynamic picture’ and so accept points **(a)** and **(b)**; but we aim to improve upon **(c)**. Indeed, the cubic form of $h(M)$ is inextricably linked to the classical critical exponent values $\beta = \frac{1}{2}$, $\gamma = 1$, $\delta = 3$, etc. Naturally, we hope that, in some sense, we are not merely asking: ‘How many angels can dance on the head of a pin?’. In any event, we will provide reasonable expressions for loop profiles $h(M)$ consistent with nonclassical behaviour thereby providing a satisfactory basis for better phenomenological theories of surface tensions near critical endpoints [4, 9–11], of critical adsorption [12, 13], and of compositional profiles between walls with competing boundary conditions [13, 14], etc.

To represent our results for the vdW loops, scaled versions of M and h are desirable. Accordingly, for $T < T_c$, we introduce

$$\tilde{m} \equiv M/M_0(T) \approx M/B|t|^\beta \quad \text{and} \quad \tilde{h} \equiv h/[M_0(T)/\chi_0(T^+)] \approx C^+h/B|t|^{\beta+\gamma}. \quad (1)$$

The definition of \tilde{m} is natural, the coexistence curve being specified simply by $\tilde{m} = \pm 1$. To define \tilde{h} we have invoked the zero-field susceptibility, $\chi_0 = (\partial M/\partial h)_{h \rightarrow 0}$, evaluated at the complementary temperature, $T^+ = (1 + |t|)T_c$, *above* criticality. This varies (see the appendix) as $C^+/|t|^\gamma$ and is appropriate for scaling since the susceptibility and its amplitude are both more fundamental and more accessible to experimental observation, to simulation [15, 16], to numerical estimation [17–21], and to RG analysis, etc [21–23], *above* T_c than below T_c . (Note that the references cited here are meant only to be representative of recent work and of relevance to table 1.) As a result of (1), slopes on an (\tilde{m}, \tilde{h}) plot, as in figure 1, are measured on the scale $1/\chi_0(T^+)$. By the same token, an (\tilde{m}, \tilde{h}) plot *above* T_c (with M_0 evaluated at $T^- = (1 - |t|)T_c$) has a slope of unity at the origin.

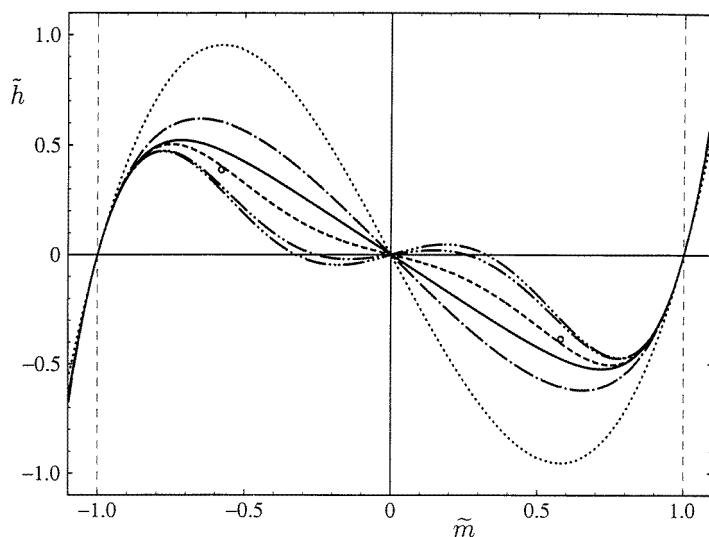


Figure 1. Scaled vdW loops predicted by low-order Padé approximants, $[L/M]$, to $u(\tilde{m}^2)$ in (2) utilizing the universal amplitude ratios U_2 , R_3 and R_4 : see table 1. The broken vertical lines at $\tilde{m} \equiv M/M_0(T) = \pm 1$ indicate the limits of the two-phase region. From the top downwards on the left plots are: dotted, [0/0]; chain [0/1]; full, [0/2]; broken, [1/0]; double chain, [2/0]; and triple chain, [1/1]. The open circles locate the classically predicted spinodal points: these do *not* lie on the cubic approximant [0/0] because of the incorrect classical value $U_2 \equiv C^+/C^- = 2$.

Table 1. Universal critical amplitude ratios. The amplitudes, A^\pm , B , etc, are defined in the appendix. The uncertainties indicated for the selected estimates for the ($d = 3$)-dimensional Ising (or $n = 1$) universality class refer to the last decimal place quoted. The scaling and hyperscaling exponent relations $\gamma = (2 - \eta)v$, $2 - \alpha = 2\beta + \gamma = \beta(\delta + 1) = \beta + \Delta = dv$ and $\mu = (d - 1)v$, are assumed and the values $\gamma = 1.2392 \pm 3$ and $v = 0.6308 \pm 12$ have been accepted (although, within the quoted uncertainties, most ratios are not sensitive to these exponent estimates). Note that the *renormalized coupling constants*, g_+^* and g_-^* , can be derived from R_4 and R_3 , etc: see [18, 19] and [g] below.

$U_0 \equiv A^+/A^-$	0.523 ± 9	[a]
$U_2 \equiv C^+/C^-$	4.95 ± 15	[a,b]
$U_4 \equiv C_4^+/C_4^-$	-9.0 ± 3	[c,g]
$R_c \equiv \alpha A^+ C^+ / B^2$	0.0581 ± 10	[a]
$R_0 \equiv (C_4^+)^2 / C^+ C_6^+$	0.1275 ± 3	[c]
$R_3 \equiv -C_3^- B / (C^-)^2$	6.44 ± 30	[c,e,g]
$R_4 \equiv C_4^- B^2 / (C^-)^3$	107 ± 13	[c,g]
$R_4^+ \equiv C_4^+ B^2 / (C^+)^3$	7.94 ± 12	[e,f]
$Q_1 \equiv C^c \delta / (B^{\delta-1} C^+)^{1/\delta}$	$0.91 \pm 2_5$	[d,e]
$Q_1^{-\delta} \equiv DC^+ B^{\delta-1}$	1.57 ± 23	[f]
$U_\xi \equiv \xi_{1,0}^+ / \xi_{1,0}^-$	1.96 ± 1	[a]
$Q_2 \equiv (\xi_{1,0}^+ / \xi_{1,0}^-)^{2-\eta} (C^+ / C^c)$	1.17 ± 2	[d]
$Q^+ \equiv \alpha A^+ (\xi_{1,0}^+)^d$	$0.0188 \pm 1_5$	[a]
$Q_c \equiv Q^+ / R_c \equiv (\xi_{1,0}^+)^d B^2 / C^+$	$0.323_6 \pm 6$	[e,f]
$Q^- \equiv \alpha A^- (\xi_{1,0}^-)^d$	$0.0047_7 \pm 2$	[e]
$Q_\xi^+ \equiv \xi_0^+ / \xi_{1,0}^+$	1.0001	[e]
$Q_\xi^- \equiv \xi_0^- / \xi_{1,0}^-$	1.037 ± 3	[e,b]
$Q_\xi^c \equiv \xi_0^c / \xi_{1,0}^c$	1.007 ± 3	[e]
$S^- \equiv \bar{K} (\xi_{1,0}^-)^{d-1}$	0.098 ± 2	[d,e]
$S^+ \equiv \bar{K} (\xi_{1,0}^+)^{d-1}$	0.377 ± 11	[e]
$S_0 \equiv \bar{K} C^+ / B^2 \xi_{1,0}^+$	1.17 ± 6	[e,f]

[a] See [17]. [b] Caselle and Hasenbusch [15] in a carefully analysed Monte Carlo study, adopted essentially the same values of γ and v and concluded $U_2 \equiv C^+/C^- = 4.75 \pm 6$, $U_\xi \equiv \xi_{1,0}^+ / \xi_{1,0}^- = 1.95 \pm 4$, and $Q_\xi^- \equiv \xi_0^- / \xi_{1,0}^- = 1.017 \pm 14$ (where their quoted statistical errors have been doubled): only the ratio U_2 can be considered significantly lower than listed here. [c] See [18]. [d] See [19]. [e] See Zinn [11, chapter 2]; but note that, as regards Q_1 and R_3 , the work of Guida and Zinn-Justin [22] is now taken into account. Likewise, for S^- , S^+ and S_0 , the surface tension amplitude \bar{K} has been revised using Hasenbusch and Pinn [16]. [f] Derived by combining primary estimates listed above in the table. [g] The ratios U_4 , R_3 and R_4 enter into expressions for the renormalized coupling constants via $g_+^* \equiv -C_4^+ / (C^+)^2 (\xi_{1,0}^+)^d = -R_4 U_4 / U_3^3 Q_c$ and $g_-^* = (3R_3^2 - R_4) U_\xi^2 / U_2 Q_c$. The central estimates listed yield $g_+^* \simeq 24.54$ compared with 24.45 ± 15 as estimated in [18]. However, the more recent analysis of Guida and Zinn-Justin [22] leads to 23.70 ± 10 which is supported by studies of Butera and Comi and of Pelissetto and Vicari (the latter obtaining 23.55 ± 24). If such lower estimates hold up, the central values of U_4 and R_4 may need adjustment (although probably remaining within the ranges quoted). Owing to cancellations between large terms, $g_-^* \simeq 85$ [11, 18] is difficult to estimate: future more reliable estimates should yield refined values also for R_3 .

In terms of \tilde{m} and \tilde{h} one expects the vdW loop (and associated stable isotherms) to take the asymptotic scaling form

$$\tilde{h} = \tilde{m}(\tilde{m}^2 - 1)u(\tilde{m}^2) \quad (t \rightarrow 0-) \quad (2)$$

where $u(y)$ is a *universal* function that we seek. Classically one then has $u \equiv 1$; more

generally, for a properly shaped loop, one needs $u(0), u(1) > 0$. Now, by employing the universal amplitude ratios defined in table 1 (in terms of the critical amplitudes given in the appendix), the order parameter near criticality may be expanded in powers of $\tilde{h} \rightarrow 0 \pm$ as

$$\tilde{m} = \pm 1 + (\tilde{h}/U_2) \mp \frac{1}{2}R_3(\tilde{h}/U_2)^2 + \frac{1}{6}R_4(\tilde{h}/U_2)^3 \mp \dots \quad (3)$$

Obviously, the analytic continuation of these series truncated at some available order will *not* produce a sensible vdW loop inside the two-phase region. Instead, let us construct Padé approximants, $[L/M]$, to $u(y)$ that, on inversion of (2), match the expansion (3) to desired order. The simplest approximant is $[0/0] = \frac{1}{2}U_2 \equiv \frac{1}{2}(C^+/C^-)$; others are readily found (see [11], table 3.2). The resulting predictions for the vdW loop are shown in figure 1 where the values of U_2, R_3 , and R_4 in table 1 have been used. Many of the loops are quite anomalous, with unexpected points of inflection, etc. A highest order approximant, matching all terms displayed in (3), is

$$u_{[0/2]}(1+z) = U_2/2\{1 - \frac{1}{4}(R_3 - 3)z - \frac{1}{48}[3(1 + R_3)^2 - 2R_4]z^2\}. \quad (4)$$

Since the two other approximants of this order, $[1/1]$ and $[2/0]$, yield loops with extra zeros (see figure 1) they may be regarded as ‘defective’. Thus the estimate (4) for $u(\tilde{m}^2)$ is to be favoured; but we can do better.

To deal effectively with nonclassical equations of state, parametric representations [24–27] are essential. Ideally [4], the vdW loop would follow simply by analytic continuation of the parametric equations into the two-phase regions. However, as noted previously [4], the well known *linear model* [24,25] *fails* to generate a real, complete vdW loop. The same is true of the *cubic model* [27,11] and its extensions [11,28]. To overcome this

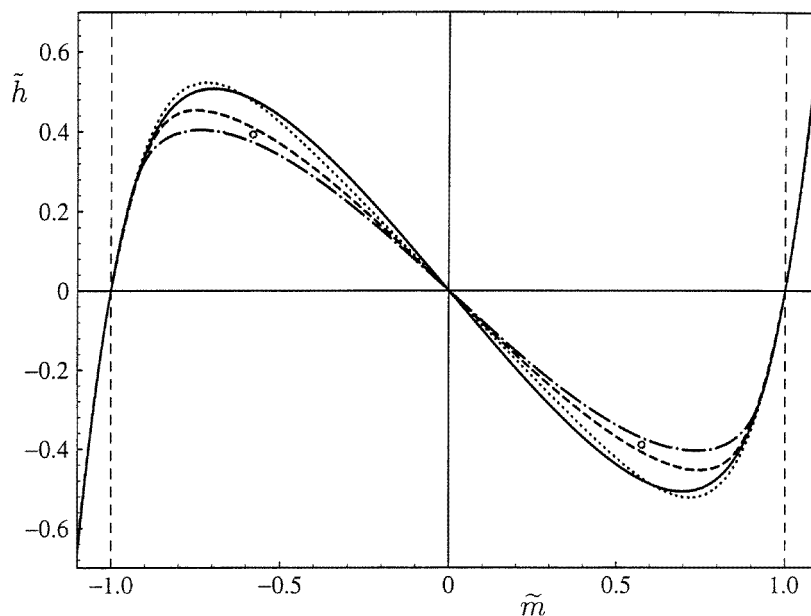


Figure 2. Estimates for the scaled vdW loop: (a) the *full curve*, based on the extended sine model, is preferred. (b) The dotted curve, which approximates (a) reasonably well, is the $[0/2]$ approximant, also shown in figure 1: see (4). The (c) broken and (d) chain curves represent the extended cubic model and the linear model (with $b = 1.25$) respectively, both interpolated to order $N = 2$. The open circles again locate the spinodal points predicted classically.

Table 2. Estimates for universal vdW loop parameters. For definitions and explanations, see text. The predictions of the extended sine model (in the last row) are preferred. The uncertainties quoted refer to the last decimal place.

	\tilde{m}_s	\tilde{h}_s	$1 - (A^*/A^-)$	C^-/C^*
Classical vdW results				
	$\frac{1}{\sqrt{3}} \simeq 0.577$	$-\frac{2\sqrt{3}}{9} \simeq -0.385$	1	$-\frac{1}{2}$
Padé approximants [L/M]				
[0/0]	$\frac{1}{\sqrt{3}}$	-0.953 ± 29	0.984 ± 64	$-\frac{1}{2}$
[1/0]	0.749 ± 15	-0.507 ± 42	0.420 ± 76	-0.070 ± 38
[0/1]	$0.653_7 \pm 5$	-0.621 ± 37	0.637 ± 60	-0.269 ± 11
[2/0]	0.779^{+49}_{-201}	-0.471^{+75}_{-205}	0.29 ± 42	0.060 ± 44
[1/1]	0.783 ± 90	-0.467 ± 12	0.25^{+38}_{-210}	0.12^{+560}_{-140}
[0/2]	0.719 ± 40	-0.521 ± 70	0.506^{+125}_{-87}	-0.175^{+36}_{-62}
Interpolated linear model ($b = 1.250$)				
$N = 1$	0.700 249	-0.411 925	0.466 739	-0.168 487
$N = 2$	0.736 378	-0.404 349	0.455 206	-0.156 315
Interpolated extended cubic model				
$N = 1$	0.713 ± 3	-0.461 ± 2	0.477 ± 5	-0.185 ± 2
$N = 2$	0.746 ± 5	-0.454 ± 2	0.462 ± 3	-0.171 ± 3
Extended sine model				
	0.697 ± 2	-0.513 ± 20	0.514 ± 8	-0.205 ± 3

difficulty, Fisher and Upton [4] proposed interpolation through the two-phase region (using a low-order polynomial in a complementary parametric angle, $\bar{\theta}$) while matching the value of M and the first N derivatives, $(\partial^k M / \partial h^k)$, on the coexistence curve.

The chain and broken curves in figure 2 show the resulting $N = 2$ interpolations [11] for the linear model and (an extended) cubic model, respectively, when these are fitted (as best possible) to the data of table 1 [11, 28]. Note that the dotted curve represents the [0/2] approximant (4), which, in fact, also fits $(\partial^3 M / \partial h^3)$. This interpolation scheme is reasonable but rather *ad hoc*. Furthermore, the $(k > N)$ th derivatives are discontinuous at the coexistence curve and the results must fail at some point when N is increased since they will approach the (inadequate) analytic continuation.

As an attractive alternative, Fisher and Upton proposed a trigonometric or *sine model* [4, 26] which, by construction, always provides a complete, real analytic continuation through the two-phase region. Such representations have now been studied [11, 28]. In order to fit the data in table 1 satisfactorily it proves both necessary and beneficial to parametrize the singular part of the reduced canonical free energy, $\mathcal{A}(T, M)$, directly (rather than the equation of state, as is traditional [24–27]). In brief, we write

$$t = rk(\theta) \quad M = r^\beta m(\theta) \quad h = r^{\beta\delta} l(\theta) \quad \mathcal{A}_s(T, M) = r^{2-\alpha} n(\theta) \quad (5)$$

where, omitting regular terms, $\mathcal{A}_s(T, M) = \int^M h(M'; T) dM'$. Then we adopt [4, 11, 28]

$$k(\theta) = 1 + k_1[\cos(q\theta) - 1] \quad m(\theta) = m_0 \sin(q\theta)/q \quad n(\theta) = \sum_{j=0}^4 n_j k^j(\theta) \quad (6)$$

for $|\theta| \leq \theta_0 = \pi/q$, in which m_0 and n_0 serve as unimportant metrical factors while $k_1 \equiv 2b^2/q^2 > 0$, q , and n_1 to n_4 constitute six parameters. These may be adjusted to provide good fits [11, 28] to the eight independent universal thermodynamic ratios, U_0 to

Q_1 , listed in table 1. (The remaining, correlation length and surface tension, ratios are included for reference since they are also required for applications of the nonclassical local functional theories [4, 10, 13].)

By these means the full curve in figure 2 has been calculated [11, 28]. Since it meets the original requirements **(a)** and **(b)**, and fits all currently available critical data, we regard it as the optimal prediction for the scaled van der Waals loop. Evidently, it is not too badly approximated numerically by the [0/2] approximant (4). However, to be more quantitative, we present in table 2 a list of universal shape parameters characterizing the loop. These are: first, the values, $\pm\tilde{m}_s$ and $\pm\tilde{h}_s$, of \tilde{m} and \tilde{h} on the spinodals; then, the *slope ratio*, C^-/C^* , where the ‘unstable (negative) susceptibility’, $\chi^* \equiv (\partial M/\partial h)_{M \rightarrow 0}$ below T_c varies as $C^*/|t|^\nu$, and, last, the *scaled free energy barrier*, $1-(A^*/A^-)$, which represents the height of the free energy maximum at $M = 0$ below T_c relative to the minima at $M = \pm M_0(T)$. This parameter thus measures the area under one lobe of the vdW loop and follows, more concretely, from $C^*(T)$, the $M = 0$ specific heat below T_c , which varies as $A^*/|t|^\alpha$.

It is clear from table 2, as from the figures, that the shape of any plausible vdW loop for a three-dimensional system near criticality, differs significantly from the classical form. In particular, the spinodal should be further out (i.e. closer to the binodal or coexistence curve) and the ‘size’ of the loop, as measured by the area under its lobes and the central slope, must be smaller by a factor of about 2 or more. In addition to the applications already mentioned [3, 4, 10, 12, 13], these results may be useful in studies of spinodal decomposition near criticality and in other problems where interface profiles need to be modelled.

Informative communications from M Hasenbusch, K Pinn, J Zinn-Justin, P Butera, M Comi, A Pelissetto, A I Sokolov and D P Landau, have been appreciated. The authors are grateful for the inspiration provided by Ben Widom and by earlier work of Paul J Upton, and for the support of the National Science Foundation (through grants CHE 93-11729 and 96-14495).

Appendix. Definitions of critical amplitudes

We define the reduced free energy density (or pressure) for a system of volume V as a function of *thermodynamic fields*, T and h , via $\bar{f} = -F/Vk_B T = V^{-1} \ln Z(T, h)$ where the partition function is $Z = \text{Tr}\{\exp(\bar{\mathcal{H}})\}$ with a reduced Hamiltonian of the form

$$\bar{\mathcal{H}} = -\mathcal{H}/k_B T = \bar{\mathcal{H}}_0 + h \int M(\mathbf{r}) \, d\mathbf{r} \quad (\text{A1})$$

where $\int d\mathbf{r}$ is replaced by $\sum_{\mathbf{R}} v_0$ in a lattice system with cell volume v_0 , the *order parameter density*, $M(\mathbf{r})$, being then defined only at lattice sites, \mathbf{R} . In magnetic systems $M(\mathbf{r})$ may be the spin density and one then has $h = \mu_0 H/k_B T$, where H is the magnetic field and μ_0 is a unit magnetic moment; for fluids $M(\mathbf{r})$ may be a number (or mass) density deviation in which case one has $h = \mu/k_B T$ (or $\mu/m_0 k_B T$), where μ is the chemical potential (or a chemical potential difference, while m_0 sets a suitable molecular mass scale). Other thermodynamic fields, such as an overall pressure, are understood to be held constant.

To describe critical behaviour, we set $T = T_c(1 + t)$ and suppose $h_c = 0$ and $M_c = 0$: thus for a fluid, one may take $M = \rho - \rho_c$, where ρ is the number or mass density, etc. To specify critical amplitudes on the ‘critical isochore’ $M = M_c$ above T_c , or at coexistence below T_c (assuming asymptotic symmetry under $M \Leftrightarrow -M$), we write the reduced specific heat and spontaneous order (or coexistence curve) as

$$C(T) = (\partial^2 \bar{f} / \partial t^2) \approx A^\pm / |t|^\alpha \quad M_0(T) = (\partial \bar{f} / \partial h)_{0+} \approx B |t|^\beta \quad (\text{A2})$$

when $t \rightarrow 0\pm$, and the susceptibilities as

$$\chi(T) = (\partial M / \partial h)_0 \approx C^\pm / |t|^\gamma \quad \chi_k(T) = (\partial^k \bar{f} / \partial h^k)_0 \approx C_k^\pm / |t|^{\gamma + (k-2)\Delta} \quad (\text{A3})$$

where scaling for field derivatives ($k > 2$) has been assumed as well as equality of exponents for $t \gtrsim 0$. The second-moment and true correlation lengths vary as

$$\xi_1(T) \approx \xi_{1,0}^\pm / |t|^\nu \quad \xi_\infty(T) \approx \xi_0^\pm / |t|^\nu \quad (\text{A4})$$

when $t \rightarrow 0\pm$. (In systems with lattice spacing a we write $\xi_{1,0}^+ = f_1^+ a$, etc [17].) For the interfacial tension, $\Sigma(T)$, between coexisting phases, amplitudes are defined by

$$\Sigma(T) \approx K |t|^\mu \quad \text{when } t \rightarrow 0 - \quad \text{and} \quad \bar{K} \equiv K / k_B T_c. \quad (\text{A5})$$

Finally, on the *critical isotherm*, $T = T_c$, we take $\gamma_c = 1 - (1/\delta)$ and

$$h \approx \pm D |M|^\delta \quad \chi(h) \approx C^c / |h|^{\gamma_c} \quad \xi_1(h) \approx \xi_{1,0}^c / |h|^{\nu_c} \quad \xi_\infty(h) \approx \xi_0^c / |h|^{\nu_c} \quad (\text{A6})$$

so that $C^c = 1/\delta D^{1/\delta}$, while scaling dictates $\delta = \Delta/\beta$, $\gamma_c = \gamma/\Delta$, $\nu_c = \nu/\Delta$, $\Delta = \beta + \gamma$, $\alpha + 2\beta + \gamma = 2$, etc. Hyperscaling, which is assumed in the last two sections of table 1, gives $\mu = (d-1)\nu$ and $2 - \alpha = d\nu$, etc.

References

- [1] Rowlinson J S and Widom B 1982 *Molecular Theory of Capillarity* (London: Oxford University Press)
- [2] Cahn J W and Hilliard J E 1958 *J. Chem. Phys.* **28** 258
- [3] Ramos-Gómez F and Widom B 1980 *Physica* **104A** 595
- [4] Fisher M E and Upton P J 1990 *Phys. Rev. Lett.* **65** 3405
Fisher M E and Upton P J in preparation
- [5] Fisher M E and Felderhof B U 1970 *Ann. Phys., NY* **58** 176
Fisher M E and Felderhof B U 1970 *Ann. Phys., NY* **58** 217
- [6] Fisher M E 1967 *Physics* **3** 255
- [7] Andreev A F 1964 *Sov. Phys.-JETP* **18** 1415
- [8] Isakov S N 1984 *Commun. Math. Phys.* **95** 427
- [9] Fisher M E and Upton P J 1990 *Phys. Rev. Lett.* **65** 2402
Fisher M E 1991 *Physica* **172A** 77
- [10] Zinn S-Y and Fisher M E in preparation
- [11] Zinn S-Y 1997 *PhD Thesis* University of Maryland, College Park
- [12] Liu A J and Fisher M E 1989 *Phys. Rev. A* **40** 7202
- [13] Upton P J 1992 *Phys. Rev. B* **45** 8100
Upton P J and Borjan Z in preparation
- [14] Fisher M E and Au-Yang H 1980 *Physica* **101A** 255
- [15] Caselle M and Hasenbusch M 1997 *J. Phys. A: Math. Gen.* **30** 4963
- [16] Hasenbusch M and Pinn K 1997 *Physica* **245A** 366
- [17] Liu A J and Fisher M E 1989 *Physica* **156A** 35
- [18] Zinn S-Y, Lai S-N and Fisher M E 1996 *Phys. Rev. E* **54** 1176
- [19] Zinn S-Y and Fisher M E 1996 *Physica* **226A** 168
- [20] Butera P and Comi M 1997 *Phys. Rev. B* **56** 8212
- [21] Campostrini M, Pelissetto A, Rossi P and Vicari E 1998 *Phys. Rev. E* **57** 184
- [22] Guida R and Zinn-Justin J 1997 *Nucl. Phys. B* **489** [FS]626
- [23] Sokolov A I, Ul'kov V A and Orlov E V 1997 *J. Phys. Studies* **1** 1
- [24] Schofield P 1969 *Phys. Rev. Lett.* **22** 606
- [25] Schofield P, Litster J D and Ho J T 1969 *Phys. Rev. Lett.* **23** 1098
- [26] Fisher M E 1971 *Critical Phenomena* ed M S Green (New York: Academic) p 35 *et seq*
- [27] Tarko H B and Fisher M E 1973 *Phys. Rev. Lett.* **31** 926
Tarko H B and Fisher M E 1975 *Phys. Rev. B* **11** 1217
- [28] Zinn S-Y, Fisher M E and Upton P J in preparation